Energy Proceedings
Vol 44, 2024
ISSN 2004-2965

Multi-optimization of carbon capture by temperature swing adsorption based on artificial neural network surrogate model

Qi Zhang[1], Shuai Deng[1*], Ruikai Zhao[1], Bingyang Zhang[2]

1 Key Laboratory of Efficient Utilization of Low and Medium Grade Energy (Tianjin University), Ministry of Education of China, Tianjin 300350, China

2 School of Environment Science and Engineering (Tianjin University), China, Tianjin 300350, China
(*Corresponding Author: sdeng@tju.edu.cn)

ABSTRACT

The increase in CO_2 emissions has led to a series of environmental problems, including global warming, making it imperative to reduce CO_2 emissions. Adsorption carbon capture technologies have been widely researched, but there is currently a lack of comprehensive research on the optimization of cyclic performance that considers multiple objectives. This paper focuses on temperature swing adsorption (TSA) and develops algorithms for cyclic performance optimization. It employs machine learning techniques to conduct multi-objective optimization of the cycle. The calculation time for the surrogate model is only 1/1000 of the TSA mathematical model. The results indicate that the surrogate model obtained through machine learning accurately represents the cyclic performance under different operating parameters. There is a competitive relationship between productivity and exergy efficiency throughout the cycle. Recovery rate and exergy efficiency exhibit a dual relationship, both competitive and positively correlated. Purity and recovery rate show a purely positive relationship.

Keywords: CO_2, TSA, cycle performance, cycle optimization, cycle decision-making

NONMENCLATURE

Abbreviations	
ANN	artificial neural network
CCS	carbon capture and storage
GA	genetic algorithm
TSA	temperature swing adsorption
Symbols	
Pr	Productivity
Pur	Purity
Re	Recovery rate

1. INTRODUCTION

Over the past few decades, due to extensive human use of fossil fuels, CO_2 emissions have surged dramatically, leading to consistently high levels of CO_2 concentration in the atmosphere. Reducing CO_2 emissions has become a responsibility that all countries must bear. Among various technologies, carbon capture and storage (CCS) is considered a crucial technology capable of both reducing CO_2 emissions and decreasing existing CO_2 concentrations [[1]. CCS technologies encompass methods such as absorption, adsorption, membrane separation, and more. Among these, adsorption-based carbon capture has garnered attention from researchers due to its advantages, such as its ease of integration with real carbon sources and renewable energy sources, and it has witnessed rapid development over the past few decades [2,3].

There remains a gap between the performance of adsorption-based recovery cycles and the commercial standards required, including various performance metrics such as overall energy consumption, product gas yield, and purity [4]. Factors influencing the performance of adsorption cycles primarily fall into two categories: the choice of adsorbent material [5,6] and the configuration of the cycle [7]. Among these factors, the cycle configuration is of paramount importance and is notably intricate and subject to widespread investigation. In much of the previous research on cycle performance, attention has not been directed toward the multi-objective optimization of cycle performance considering the interplay of multiple factors [8,9]. However, previous studies have indicated that employing multi-objective optimization methods to explore the relationships among cycle performance

This is a paper for 15th International Conference on Applied Energy (ICAE2023), Dec. 3-7, 2023, Doha, Qatar.

indicators can yield optimal operating conditions, which hold significant importance for cycle design [10].

This study focuses on temperature swing adsorption (TSA) which is more compatible with low-temperature waste heat. It involves the establishment of a cyclic computational model and a system of performance evaluation indicators. Employing machine learning techniques, surrogate functions are generated to represent the relationships between cycle performance indicators and cycle operating parameters. These surrogate functions, combined with cycle performance optimization algorithms, enable the rapid multi-objective optimization of cycle performance, accommodating up to four objectives.

Furthermore, based on the weighting requirements of the cycle performance indicators, decisions are made regarding the optimal performance of the cycle and the corresponding cycle operating parameters. This facilitates the fulfillment of diverse production demands.

2. METHOD

2.1 Adsorbents and equilibrium isotherms

This article regards the waste gas to be recovered as a binary mixture of CO_2 and N_2 [11]. The adsorbent material used in the research case is Mg-MOF-74, which is one of the materials with excellent CO_2 separation performance in metal-organic frameworks (MOFs). [12]. The adsorption equilibrium isotherms of this adsorbent for CO_2 and N_2 follow the Toth model form, as shown in Eq. (1) and Eq. (2).

$$q_k^* = \frac{q_{m,k} K_{eq,k} y_k p}{\left(1 + (K_{eq,k} y_k p)^{n_k}\right)^{\frac{1}{n_k}}} \tag{1}$$

$$K_{eq,k} = K_{0,k} \exp\left(-\frac{\Delta H_k}{RT}\right) \tag{2}$$

The relevant parameters of the Toth model are from reference [13].

2.2 Temperature swing adsorption cycle model

The TSA cycle is the process of using adsorbents to adsorb at lower temperatures and desorb adsorbed gases at higher temperatures [14], which is easy to combine with low-grade thermal energy and has economic benefits and advantages [15]. The TSA operation process studied in this article is divided into four steps: heating, cooling, pressurization, and adsorption. Figure 1 shows the four processes of TSA:

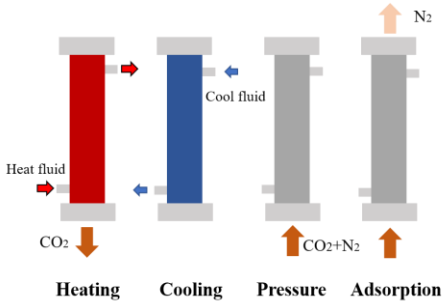

Fig.1. Four steps of the TSA cycle

In prior research, the authors established a computational model for the recovery of CO_2 and N_2 gas mixtures through a TSA cycle [16]. This model is founded on the principles of mass and energy conservation within the adsorption bed. It encompasses analytical or semi-analytical expressions tailored to the characteristics of each cycle step. With given initial and constraint conditions, this model can solve for the state parameters within the adsorption bed at each point in time. Utilizing this model, computational simulations of the TSA cycle were conducted, and the obtained state parameters were subsequently used to calculate performance evaluation indicators for the cycle.

2.3 Evaluation indicators for cycle performance

In prior research, the authors established a computational model for the recovery of CO_2 and N_2 gas mixtures through a TSA cycle [16]. This model is founded on the principles of mass and energy conservation within the adsorption bed. It encompasses analytical or semi-analytical expressions tailored to the characteristics of each cycle step. With given initial and constraint conditions, this model can solve for the state parameters within the adsorption bed at each point in time. Utilizing this model, computational simulations of the TSA cycle were conducted, and the obtained state parameters were subsequently used to calculate performance evaluation indicators for the cycle.

Productivity (Pr) represents the amount of target gas captured per unit time and unit mass of adsorbent, as shown in E. (3).

$$Pr = \frac{N_{CO_2,heat}/t_{cycle}}{\rho_b V_{col}} \tag{3}$$

Purity (Pur) represents the molar fraction of CO2 gas in the recovered product gas, as shown in Eq. (4).

$$Pur = \frac{N_{CO_2,heat}}{N_{CO_2,heat} + N_{N_2,heat}} \tag{4}$$

The recovery rate (Re) represents the capture rate of the target gas in the mixed gas by the cycle, as shown in Eq. (5).

$$Re = \frac{N_{CO_2,heat}}{N_{CO_2,in}} \quad (5)$$

Exergy efficiency (Eff) is expressed as the proportion of the minimum work for gas separation to the actual consumed thermal energy, as shown in Eq. (6).

$$Eff = \frac{W_{\min}}{Q_{TSA}\left(1 - \frac{T_L}{T_H}\right)} \quad (6)$$

2.4 Cycle performance evaluation indicators

The TSA calculation model needs to solve several differential equations, so if this model is brought into the cyclic optimization algorithm, the optimization process will take a long time, and other problems will easily appear in the calculation process. Therefore, this paper uses the machine learning method to get a substitute model and uses it to replace the TSA calculation model of cyclic performance index calculation in the optimization process. The substitution model is an alternative representation of the multivariable mapping structure of the input-output space constructed based on the TSA model calculation results as samples. The replacement model does not need to solve the differential equations repeatedly, so its combination with the optimization algorithm can significantly reduce the computational cost. Among many methods, artificial neural network (ANN), Kriging method, support vector regression, and response surface method are the most popular technologies [17]. In this study, artificial neural network methods are used to construct alternative models. After calculating enough sample data, the neural network model is built using MATLAB, and the Levenberg-Marquardt algorithm is used to solve the model instead.

2.4 Genetic algorithm for multi-objective optimization

Genetic algorithm (GA) is a mature multi-objective optimization tool that can serve as a method for loop optimization. A genetic algorithm is an evolutionary optimization algorithm that starts from an individual population and improves the value of the objective function through repeated screening processes across multiple generations [18]. This article uses a genetic algorithm combined with a substitute model to achieve multi-objective optimization with the established loop performance indicators as the goal. This article has successively considered the three objective optimization problems of Pr, Re, Eff, and the four objective optimization problems of Pr, Pur, Re, Eff. The above two multi-objective optimization problems are equivalent to the problems shown in equations (7) and (8).

$$\max\begin{pmatrix} Pr \\ Re \\ Eff \end{pmatrix} = F(T_L, T_H, p, y_{in})$$
$$s.t.\begin{cases} T_{L\min} \le T_L \le T_{L\max} \\ T_{H\min} \le T_H \le T_{H\max} \\ p_{\min} \le p \le p_{\max} \\ y_{in\min} \le y_{in} \le y_{in\max} \end{cases} \quad (7)$$

$$\max\begin{pmatrix} Pr \\ Re \\ Pur \\ Eff \end{pmatrix} = F(T_L, T_H, p, y_{in})$$
$$s.t.\begin{cases} T_{L\min} \le T_L \le T_{L\max} \\ T_{H\min} \le T_H \le T_{H\max} \\ p_{\min} \le p \le p_{\max} \\ y_{in\min} \le y_{in} \le y_{in\max} \end{cases} \quad (8)$$

In the Eq. (7) and Eq. (8), F represents the substitute model function. The optimization range of various operating conditions parameters is shown in Table 1.

Table. 1. The research scope of working parameters

	T_L	T_H	P	y_{in}
Upper Bound	313K	440K	4bar	0.2
Lower Bound	273K	330K	1bar	0.05

3. RESULTS AND DISCUSSIONS

3.1 ANN-based model

Using the TSA calculation model established above, the cyclic performance indicators under the operating conditions within the range of Table 2 were calculated. Using the method of controlling variables, 11 gradients were selected within each operating parameter range, and the combined operating conditions were arranged in a cross manner. A total of 14642 sets of operating conditions parameters were selected, and their corresponding cyclic performance indicator values were obtained. Use the obtained data for the construction of the ANN function. Among them, there are 4 input variables and 4 output variables. 20 neurons were selected for construction, with 70% of the data used for training, 15% for verification, and 15% for testing. More than 98% of the calculated results of the final ANN function have data errors below 0.1, and the R2 of the fitting results is above 0.99999. There is no overfitting phenomenon, indicating that this substitute model can accurately replace the calculation results of the detailed model.

Table. 2. Comparison of calculation time

Type of model	Solution time
TSA mathematical model	1.0×10^6 s
ANN-based model	43s – 504s

The two models are used to solve the performance parameters under different working conditions. Compared with the mathematical model of TSA, the time required for solving the ANN-based model can be less than 50s.

3.2 Analysis of the relationship between cycle performance indicators

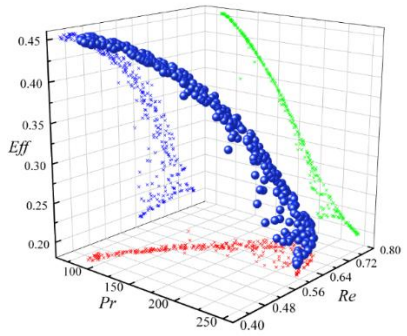

Fig.2. The 3-dimensional Pareto front and its projection for the cyclic performance index

In the Pareto optimal solution set, Pr and Re generally exhibit a positive correlation before competition. As Pr values increase, Re values will first increase synchronously. However, when the Pr value exceeds 200, further increasing the Pr value will cause a rapid decrease in the Re value. There is a competitive relationship between Pr and Eff throughout the process. As the Pr value decreases, the Eff value will increase, but the increased marginal benefit shows a result of first increasing and then decreasing. There is a dual relationship between Re and Eff that is both competitive and positively correlated, depending on the value of Eff. When Eff is less than 0.225, as Re increases, Eff will increase slightly. When Eff is greater than 0.025, Eff will significantly decrease with the increase of Re.

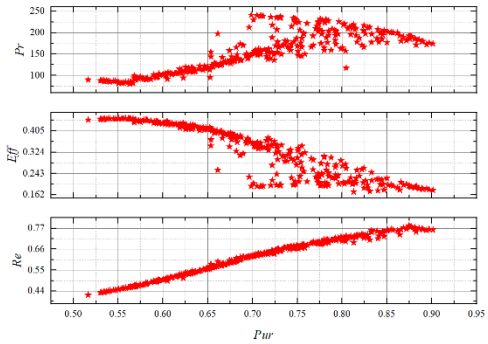

Fig.3. Relationship between Pur and other performance indicators

From the graph, it can be seen that in the Pareto solution set, there is a complete positive relationship between Pur and Re, while Pur and Eff exhibit a complete competitive relationship. There is a dual relationship between competition and a positive correlation between Pur and Pr. When Pr is greater than 200, the Pr value decreases as Pur increases. When Pr value is less than 200, the situation is exactly the opposite.

3.3 Analysis of optimal operating conditions parameters

The values of the operating conditions parameters correspond to the Pareto front in the case of three objective optimizations. From Figure 4 (a), it can be seen that the optimal operating condition parameter set almost includes all T_H values within the given range, indicating that blindly increasing T_H values cannot optimize cycle performance. In the optimal working condition parameter set, increasing T_H will cause Re to first increase and then decrease; Eff will decrease with the increase of T_H; Pr shows an increasing trend throughout the entire process as T_H increases. Figure 4 (b) shows that the T_L values in the optimal operating condition parameter set are all near the lower temperature boundary. Although the results of this study indicate that the lower the adsorption temperature, the better the cycling performance, additional cooling consumption is required below the ambient temperature to maintain low temperature. Therefore, it is advisable to use environmental temperature as the adsorption temperature in practical operation. From Figure 4 (c), it can be seen that the value of P in the optimal operating condition parameter set is between 127000 and 374000 Pa, so excessive adsorption pressure will not bring sufficient performance benefits. At the same time, it should be noted that the relationship between the changes in P and the changes in various cycle performance indicators is relatively complex, and there is no obvious pattern to follow. Overall, adopting environmental pressure for adsorption pressure is a desirable behavior, as it does not incur compressor power consumption to maintain pressure. In Figure 4 (d), it can be seen that the values of Re and Pr corresponding to the intake concentration of 0.15 to 0.2 are relatively high, and considerable Eff values can also be achieved. However, it should be noted that the y_{in} value is generally determined directly by the recovered gas source and does not undergo post-processing. Therefore, the analysis of y_{in} is to distinguish the changes in cycle performance values corresponding to different gas sources.

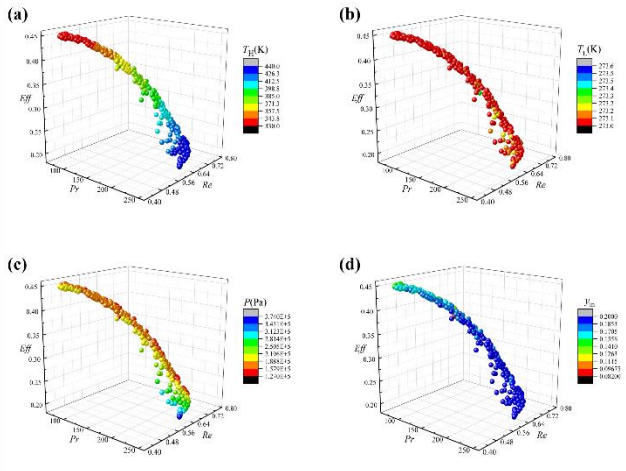

Fig.4. Pareto front corresponding to the working parameters: (a) desorption temperature (b) adsorption temperature (c) adsorption pressure (d) inlet gas concentration

For the additional results corresponding to the four objective optimization results, additional analysis is still conducted on Pur. Figure 5 shows the operating conditions parameters corresponding to Pur in the Pareto optimal solution set.

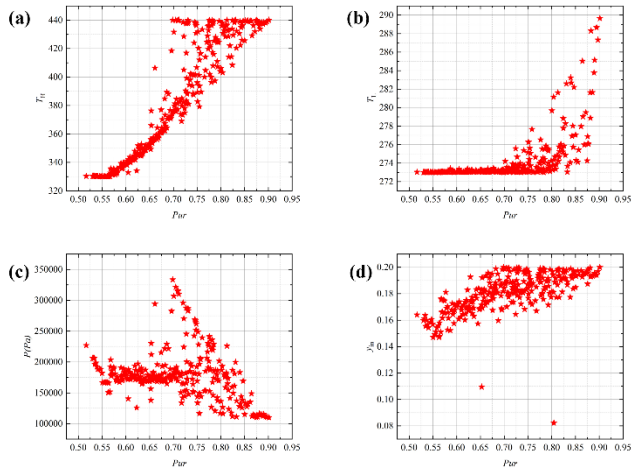

Fig.5. Pur corresponding working parameters: (a) desorption temperature (b) adsorption temperature (c) adsorption pressure (d) inlet gas concentration

From Figure 5 (a), it can be seen that increasing T_H will result in a more satisfactory Pur value. Figure 5 (b) shows that the T_L values corresponding to the optimal Pur range from 273 to 290 K, and the best Pur value is obtained when the T_L value is around 290 K. Figure 5 (c) shows that there is no obvious pattern to follow for P, but it can be seen that there is a chance to obtain the best Pur value at 101300 Pa. Figure 5 (d) shows that the y_{in} corresponding to the optimal Pur is mostly above 0.14, but in low concentrations, the cycle parameters can also be adjusted to Pur values above 0.8.

4. CONCLUSION

This paper, using the TSA cycle as an example, has established a TSA cycle performance optimization algorithm. An ANN surrogate model has been obtained through machine learning algorithms to represent the relationship between operating parameters and cycle performance. By utilizing the ANN model, along with the established multi-objective cyclic optimization algorithm and cyclic performance decision algorithm, optimization and decision-making for up to four objectives have been performed, analyzing the relationships between the optimal cyclic performance and their corresponding cycle operating parameters. The study has also analyzed cyclic performance decision-making guided by the balance of cyclic performance.

Through the research conducted, the following conclusions have been drawn:

(1) The use of machine learning algorithms to obtain an ANN surrogate model has accurately represented cyclic performance under various operating parameters. The average errors for all four cyclic performance indicators are below 5%.

(2) The Pareto-optimal solution set obtained from multi-objective optimization of the TSA cycle reveals the following relationships: Pr and Re exhibit an initial positive correlation followed by competition, Pr and Eff show a continuous competitive relationship, Re and Eff display both competition and a positive correlation, dependent on the value of Eff. Pur and Re show a complete positive correlation, while Pur and Eff exhibit complete competition. Pur and Pr demonstrate both competition and a positive correlation.

(3) The optimal operating parameter sets nearly encompass all T_H values within the given range, indicating that blindly increasing T_H values may not optimize cyclic performance. The optimal operating parameter sets have T_L values near the lower temperature boundary. The relationship between P variations and changes in various cyclic performance indicators is complex and lacks a clear pattern to follow. In the case of an inlet concentration ranging from 0.15 to 0.2, Re and Pr values are relatively high.

ACKNOWLEDGEMENT

This work is sponsored by the National Natural Science Foundation of China (No. 52306265 and No. 72104257), the Research Plan of Science and Technology of Tianjin City (No.21JCQNJC00390), and Key Project of

Natural Science Funds of Tianjin City (No. 22JCZDJC00540).

DECLARATION OF INTEREST STATEMENT

The authors declare that they have no known competing financial interests or personal relationships that could have appeared to influence the work reported in this paper. All authors read and approved the final manuscript.

REFERENCE

[1] Mai B, Adjiman C S, Bardow A, et al. Carbon capture and storage (CCS): the way forward[J]. Energy & Environmental Science, 2018(Part A).

[2] Zhao R, Liu L, Zhao L, et al. Techno-economic analysis of carbon capture from a coal-fired power plant integrating solar-assisted pressure-temperature swing adsorption (PTSA)[J]. Journal of Cleaner Production, 2019,214:440-451.

[3] Ben-Mansour R, Habib M A, Bamidele O E, et al. Carbon capture by physical adsorption: Materials, experimental investigations, and numerical modeling and simulations – A review[J]. Applied Energy, 2016,161:225-255.

[4] Khurana M, Farooq S. Adsorbent Screening for Postcombustion CO_2 Capture: A Method Relating Equilibrium Isotherm Characteristics to an Optimum Vacuum Swing Adsorption Process Performance[J]. Industrial and Engineering Chemistry Research, 2016,55(8):2447-2460.

[5] Modak A, Jana S. Advancement in porous adsorbents for post-combustion CO_2 capture[J]. Microporous and Mesoporous Materials, 2019,276:107-132.

[6] Belmabkhout Y, Guillerm V, Eddaoudi M. Low concentration CO_2 capture using physical adsorbents: Are metal–organic frameworks becoming the new benchmark materials? [J]. Chemical Engineering Journal, 2016,296:386-397.

[7] Li S, Deng S, Zhao R, et al. Entropy analysis on energy-consumption process and improvement method of temperature/vacuum swing adsorption (TVSA) cycle[J]. Energy, 2019,179:876-889.

[8] Gelles T, Lawson S, Rownaghi A A, et al. Recent advances in development of amine functionalized adsorbents for CO_2 capture[J]. Adsorption, 2019.

[9] Zhao R, Deng S, Zhao L, et al. Performance analysis of temperature swing adsorption for CO_2 capture using thermodynamic properties of adsorbed phase[J]. Applied Thermal Engineering, 2017,123:205-215.

[10] Guoxiang L, Liping P, Meng L, et al. Multiobjective Optimal Method for Carbon Dioxide Removal Assembly in Manned Spacecraft[J]. Journal of Aerospace Engineering, 2016,29(6).

[11] Joss L, Gazzani M, Hefti M, et al. Temperature swing adsorption for the recovery of the heavy component: An equilibrium-based shortcut model[J]. Industrial and Engineering Chemistry Research, 2015,54(11):3027-3038.

[12] Lian Y, Deng S, Li S, et al. Numerical analysis on CO_2 capture process of temperature swing adsorption (TSA): Optimization of reactor geometry[J]. International Journal of Greenhouse Gas Control, 2019:187-198.

[13] Ben-Mansour R, Qasem N A A. An efficient temperature swing adsorption (TSA) process for separating CO_2 from CO_2/N_2 mixture using Mg-MOF-74[J]. Energy Conversion & Management, 2018,156:10-24.

[14] Jiang L, Roskilly A P, Wang R Z. Performance exploration of temperature swing adsorption technology for carbon dioxide capture[J]. Energy Conversion & Management, 2018, 165(JUN.):396-404.

[15] Min-bae Kim, Jong-ho Moon, Chang-ha Lee, et al. Effect of heat transfer on the transient dynamics of temperature swing adsorption process[J]. Korean Journal of Chemical Engineering, 2004, 21(3):703-711.

[16] Zhao R, Liu L, Zhao L , et al. A comprehensive performance evaluation of temperature swing adsorption for post-combustion carbon dioxide capture[J]. Renewable & Sustainable Energy Reviews, 2019, 114(OCT.):109285.1-109285.13.

[17] Subraveti S G, Li Z, Prasad V, et al. Machine Learning-Based Multiobjective Optimization of Pressure Swing Adsorption[J]. Industrial & Engineering Chemistry Research, 2019,58(44):20412-20422.

[18] Maruyama R T, Pai K N, Subraveti S G, et al. Improving the performance of vacuum swing adsorption based CO_2 capture under reduced recovery requirements[J]. International Journal of Greenhouse Gas Control, 2020,93:102902.